Doxycycline reduces fibril formation in a transgenic mouse model of AL amyloidosis

Jennifer Ellis Ward,[1,2] Ruiyi Ren,[1,3] Gianluca Toraldo,[2] Pam SooHoo,[1,4] Jian Guan,[1,2] Carl O'Hara,[1,4] Ravi Jasuja,[2] Vickery Trinkaus-Randall,[1,3] Ronglih Liao,[5] Lawreen H. Connors,[1,3] and David C. Seldin[1,2]

[1]Amyloid Treatment and Research Program, and Departments of [2]Medicine, [3]Biochemistry, and [4]Pathology and Laboratory Medicine, Boston University School of Medicine and Boston Medical Center, Boston, MA, and [5]Department of Medicine, Brigham & Women's Hospital, Boston MA

Systemic AL amyloidosis results from the aggregation of an amyloidogenic immunoglobulin (Ig) light chain (LC) usually produced by a plasma cell clone in the bone marrow. AL is the most rapidly fatal of the systemic amyloidoses, as amyloid fibrils can rapidly accumulate in tissues including the heart, kidneys, autonomic or peripheral nervous systems, gastrointestinal tract, and liver. Chemotherapy is used to eradicate the cellular source of the amyloidogenic precursor. Currently, there are no therapies that target the process of LC aggregation, fibril formation, or organ damage. We developed transgenic mice expressing an amyloidogenic λ6 LC using the cytomegalovirus (CMV) promoter to circumvent the disruption of B cell development by premature expression of recombined LC. The CMV-λ6 transgenic mice develop neurologic dysfunction and Congophilic amyloid deposits in the stomach. Amyloid deposition was inhibited in vivo by the antibiotic doxycycline. In vitro studies demonstrated that doxycycline directly disrupted the formation of recombinant LC fibrils. Furthermore, treatment of ex vivo LC amyloid fibrils with doxycycline reduced the number of intact fibrils and led to the formation of large disordered aggregates. The CMV-λ6 transgenic model replicates the process of AL amyloidosis and is useful for testing the antifibril potential of orally available agents. (*Blood*. 2011;118(25):6610-6617)

Introduction

The systemic amyloidoses are a diverse group of protein misfolding diseases in which proteins aggregate and form fibrillar deposits in tissues. Amyloidosis can be genetic in origin (familial amyloidosis, AF) or can occur in the setting of chronic inflammation or infection (amyloidosis because of deposition of the acute phase serum amyloid A protein, AA). However the most commonly diagnosed form, amyloid light chain (AL) amyloidosis, is because of deposition of an immunoglobulin light chain (LC) usually produced by clonal plasma cells in the bone marrow. AL is the most rapidly fatal of the systemic amyloidoses, as LC deposits may rapidly accumulate in organs such as the heart, kidneys, autonomic or peripheral nervous systems, gastrointestinal tract, and liver.[1] Patients with AL amyloidosis are treated with chemotherapy to eradicate the plasma cell clone in the bone marrow that is the source of the amyloidogenic protein. Unfortunately, chemotherapeutics and even newer anti-plasma cell drugs with novel mechanisms of action can cause significant toxicity in AL amyloidosis patients. Although the pathophysiology of AL amyloidosis is still not completely understood, it is hoped that patient outcomes will be improved with the development of therapies that specifically target the process of protein aggregation, fibril formation, amyloid deposition, and organ damage.

Although it is clear that the overexpression of a clonal amyloidogenic LC causes AL amyloidosis, it is not clear what structural features of amyloidogenic LC are responsible for misfolding and aggregation. Furthermore, although it is well-established that glycoaminoglycans[2] and serum amyloid P component[3] can interact with LC proteins, and are found in association with amyloid fibrils, the role of these accessory molecules in fibril formation in vivo is not well understood. The role of prefibrillar LCs in organ dysfunction remains a major question in the disease pathogenesis. Data from our group have demonstrated that amyloidogenic LC can be acutely toxic to target organs, inducing oxidative stress in cells and organ culture model systems.[4,5] Amyloidogenic LCs can be internalized into cells, regulating the expression of proteoglycans and possibly mediating interactions leading to the activation of stress and other signaling pathways.[6,7] Moreover, other investigators have demonstrated that prefibrillar oligomers of other amyloidogenic proteins are cytotoxic and play an important role in amyloid pathogenesis.[8-10]

One major obstacle to understanding mechanisms of amyloid disease pathogenesis has been the lack of a genetically defined animal model. Previous animal models of AL amyloidosis have used injection of LC proteins isolated from the urine of patients with renal-involved AL amyloidosis,[11] or injection of plasmacytoma cells stably transfected with an amyloidogenic LC.[12] There are a number of disadvantages to these approaches, including the limited amount of patient-derived LC protein and temporal constraints when live plasmacytoma cells are used. Another drawback in these models is that injection or expression of a human LC in immunocompetent mice will soon lead to the development of mouse anti–human LC antibodies. This problem could be circumvented in immunocompromised mice, such as nude or $RAG^{-/-}$, but the lack of immune cells and cytokines may alter host responses normally involved in the disease process. To overcome these obstacles, we engineered a transgenic mouse expressing a human

Submitted April 28, 2011; accepted September 22, 2011. Prepublished online as *Blood* First Edition paper, October 12, 2011; DOI 10.1182/blood-2011-04-351643.

An Inside *Blood* analysis of this article appears at the front of this issue.

The publication costs of this article were defrayed in part by page charge payment. Therefore, and solely to indicate this fact, this article is hereby marked "advertisement" in accordance with 18 USC section 1734.

amyloidogenic LC, which would be recognized by the murine immune system to be endogenous and thus nonimmunogenic. The transgenic mice develop amyloid deposits, and neurologic abnormalities. These mice were used to test a potential amyloid modifying oral therapeutic, doxycycline, demonstrating the utility of this transgenic model for testing oral therapeutics.

Methods

Generation of CMV-λ6 transgenic mice. Patient samples and data were obtained from the Boston University Amyloid Treatment and Research Program repository, with written consent in accordance with the Declaration of Helsinki and with the approval of the Institutional Review Board at the Boston University Medical Center. A λ6 LC cDNA was generated by reverse transcription from RNA prepared from bone marrow collected from patient AL080 (GenBank sequence no. EF589388), who had rapidly progressive multiorgan AL amyloidosis with amyloid deposits in heart, liver, kidney, spleen, and adrenals found on autopsy. The AL080 λ6 cDNA was inserted between the *Hin*dIII and *Xba*I restriction sites in the multi-cloning region of the pcDNA3 vector (Invitrogen). A linear 2412 bp fragment of the pcDNA-AL080 λ6 plasmid containing the CMV promoter, *λ6 LC* gene, and bovine growth hormone (BGH) polyadenylation sequence was produced by restriction enzyme digestion with BglII and XmnI (NEB; Figure 1A).

Animal studies were carried out with approval of the Boston University School of Medicine Institutional Animal Care and Use Committee. Mice were housed in an Association for Assessment and Accreditation of Laboratory Animal Care–approved animal facility and maintained in a specific pathogen-free facility. Injections of pcDNA-AL080 λ6 plasmid DNA were carried out in the Boston University Medical Campus Transgenic Core Facility.

Genotyping. DNA was extracted in high salt from mouse tail or ear specimens after proteinase K digestion. Genotyping was performed by PCR amplification using a primer at the beginning of the human λ6 variable gene (5′ RATTTTATGCTGACTCAGCCCCACTCT)[13] and the end of the BGH polyadenylation region of the transgene (5′ GCCTCGACTGTGCCTTCTAGTTG). Approximately 100 ng of template DNA was amplified with the following cycles: initial denaturation at 95°C for 5 minutes, followed by 30 cycles of 95°C for 45 seconds, 54°C for 45 seconds, and 72°C for 60 seconds (iCycler, BioRad). The transgene PCR produced the expected band of 720 bp. Five potential founder mice identified by PCR were confirmed to be transgenic by Southern blot analysis of genomic DNA using 2 separate DNA probes, one spanning the variable and constant domains of the λ6 LC through the BGH polyA sequence and the other to the CMV promoter region.

Tissue protein extraction and human λ LC immunoblot. Whole cell extracts were prepared from tissues snap frozen on dry ice. Tissues were homogenized using an electric homogenizer (PowerGen 125, Fisher) in 0.5-1 mL of lysis buffer 50mM Tris-Cl pH 8.0, 1% triton X-100, 125mM NaCl, 10mM sodium pyrophosphate, 1 mM phenylmethylsulphonyl fluoride, 1mM sodium orthovanadate, 1mM sodium fluoride, 1mM EGTA, 1.5mM $MgCl_2$, 1mM DTT, 1 mg/mL aprotinin, 1 mg/mL leupeptin, 1 mg/mL pepstatin, and 0.01% protease inhibitor cocktail (Sigma-Aldrich). Homogenates were centrifuged (20 800*g*) at 4°C and total protein quantified using the BioRad Protein Assay reagent.

Immunoblots were prepared using the BioRad Mini PROTEAN II Trans-blot vertical electrophoresis and transfer apparatuses with 7.5% or 10% acrylamide gels. Separated proteins were transferred overnight to methanol activated Immobilon-P PVDF membranes (polyvinylidene difluoride, Millipore), blocked in 5% nonfat dry milk reconstituted in 1X TBS-T (50mM Tris-buffered saline (with 0.1% Tween-20) and incubated overnight with goat anti–human λ light chain (Sigma-Aldrich no. L5267, 1:2000). TBS-T washed membranes were incubated with donkey anti–goat antibody conjugated to horseradish peroxidase (HRP) secondary at 1:10 000 (Santa Cruz Biotechnology) and binding detected with enhanced chemiluminescence (West Pico, Pierce).

Laser capture microdissection. Laser capture microdissection was performed on 10 μm stomach cryosections lightly counterstained with eosin and Congo red using the Arcturus PixCell laser capture microdissection system. Amyloid deposits from 5 slides were collected per cap (Molecular Devices). The protein was solubilized from the cap using the buffer described by Gozal et al.[14] One microliter of protein extract was electrophoresed using the Phast system (Pharmacia) and silver stained (ProteoSilver Plus, Sigma-Aldrich). Approximately 9 μL of solubilized protein were electrophoresed on a 7.5% acrylamide SDS PAGE gel and immunoblotted for the human λ LC, as previously described.

Doxycycline treatment. Doxycycline (0.5 mg/mL, Sigma Chemicals) with 2% sucrose (American Bioanalytical) was provided ad libitum in red light filtering bottles and changed twice weekly. To assess the ability of doxycycline to prevent amyloid formation, we compared seventeen 3-6 month old transgenic mice given doxycycline for at least 7 months to age-matched transgenic mice (n = 16) who received only water. An equal number of line 26 treated and control and line 55 treated and control mice were used. Stomachs were bisected coronally, rinsed with 1× PBS, and a portion of the tissue was snap frozen on dry ice for protein extraction and a portion was fixed in 10% formalin for histologic analysis.

In vitro doxycycline assays. A recombinant amyloidogenic κ1 LC cloned from bone marrow plasma cells of a patient with multiorgan AL amyloidosis was prepared as previously described.[15] Recombinant LC (0.25 mg/mL) was incubated for 5 days at 37°C, alternating with cycles of at least 4 hours at 65°C, with agitation in 0.5M sodium sulfate in 10mM Tris at pH 7.4 (modified from Baden et al[16]). Doxycycline (250 mg/L or 15 mg/L) or water (control) was added at the start of the experiment and replenished after 3 days; earlier time points were studied in a second independent experiment. Proteins were visualized by negative stain electron microscopy over the time course of the incubation, as described in the next section. LC fibrils were extracted from autopsy tissue from the same patient from which the transgene was cloned,[17] lyophilized, and resuspended in saline (0.8 mg/mL). Approximately 0.5 mg/mL of fibrils were incubated in water with 0.02% sodium azide at 37°C with gentle agitation for 48 hours with 250 mg/L or 15 mg/L doxycycline or water with replenishment of doxycycline after 24 hours and then visualized by negative stain EM.

Negative stain electron microscopy. Tissue specimens of ~ 1 mm^3 were fixed in 2.5% glutaraldehyde. Before embedding, the tissues were washed with 0.2M sodium cacodylate buffer (Electron Microscopy Sciences) for 5 minutes, and post fixed with osmium tetroxide. Dehydration was performed through successive rinses in 50%, 90%, and 100% acetone. Specimen were incubated in 1:1 acetone:resin (30 mL eponate, 15 mL aradite, 55 mL DDSA, 2 mL DMP-30, Ted Pella) for 30 minutes, a fresh change of resin for 1.5 hours, and was embedded into capsules with resin. Polymerization proceeded at 60°C overnight and tissues sectioned to 0.5 μm thick. The sections were stained with 4% uranyl acetate (Fisher Scientific) for 20-30 minutes at 60°C, rinsed with distilled water, treated with lead citrate (Fisher Scientific) for 60-80 seconds, and rinsed with distilled water before observation on a transmission electron microscope (Philips 300 TEM).

Fibrils and LC treated in vitro with doxycycline were imaged by TEM on glow-discharged 300-mesh carbon-coated copper grids (Electron Microscopy Services[18]). After a 25 minute incubation on the grid, samples were negatively stained with 1% sodium phosphotungstic acid for 10 seconds. To remove excess salt before staining, grids were washed with 15 drops of distilled water or samples were washed once with distilled water before applying to the grids.

Congo red staining. Paraffin sections (7μM) were deparaffinized in xylene and rehydrated through washes of 100% and 95% ethanol followed by water. After a light counterstaining with Mayer hematoxylin, sections were incubated in an alkaline solution of salt saturated alcohol (80% ethanol, 1% sodium hydroxide, and 170mM sodium chloride) for 20 minutes followed by staining with alkaline Congo red (80% ethanol, 0.2% Congo red, and 500mM sodium chloride) for 20 minutes. Sections were dehydrated in 95%-100% ethanol and 2 xylene washes. Two sections were stained per stomach for doxycycline-treated and control mice. Photomicrography was performed using a Leica DM2000 microscope (10× or 40× objective) equipped with a Spot Insight

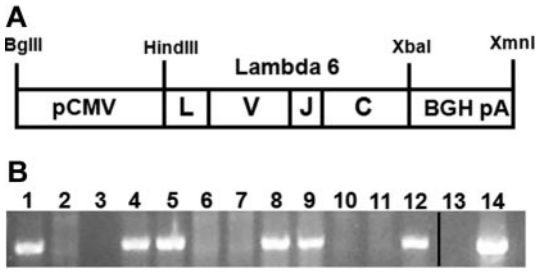

Figure 1. Schematic of the CMV-λ6 construct which is transmitted in the transgenic mouse genome. (A) The CMV-λ6 transgenic construct including the full-length immunoglobulin LC containing a leader (L), variable (V), joining (J), and constant (C) domain was expressed using the CMV promoter (pCMV) and capped with the bovine growth hormone polyadenylation sequence (BGH pA). (B) PCR genotyping of a representative litter of 10 pups (lanes 3-12) generated by crossing a transgenic line AL55 female (lane 1) and a wild-type male (lane 2) produced 50% transgene positive offspring as expected. Negative (no DNA, lane 13) and positive (plasmid DNA, lane 14) controls are present. The vertical line indicates that noncontiguous lanes from the same agarose gel image are displayed together.

2 Megasample digital camera (Model 18.2, Diagnostic Instruments) and Spot Advanced Version 4.6 software.

Immunohistochemistry. Sections (5 μm) from formalin-fixed, paraffin-embedded tissues were stained for human λ and κ (κ) LC (Dako) with the Autostainer from Dakocytomation. Briefly, endogenous peroxide reactivity was quenched with 0.3% hydrogen peroxide in methanol and antigen retrieval was performed by microwaving in Antigen Retrieval Citra Plus solution (BioGenex) for 3 and 8 minutes on high and medium, respectively. The sections were washed in wash buffer (Dako), incubated in the primary rabbit polyclonal antibody (1:25 000) in Power Block (Dako) and secondary antibody (MACH 4 universal HRP-polymer kit, Biocare Medical) and diaminobenzidine (DAB) substrate. After immunostaining, the sections were counterstained with Harris hematoxylin.

Echocardiography. The cardiac function of unanesthetized mice was assessed by echocardiography using the Acuson Sequoia C-256 echocardiograph machine and a 15-MHz probe.[19] Higher resolution echocardiography was performed on mice anesthetized with isoflurane using the VisualSonics Vevo770 micro-ultrasound imaging system. The M-mode echocardiogram was recorded at the papillary muscles of the mid-ventricle. The two-dimensional parasternal short-axis view was also imaged. The end-diastolic and end-systolic thickness of the left ventricle, interventricular septum, and posterior wall were measured, as well as heart rate. The fractional shortening of the left ventricle, calculated as the change in the end-diastolic and end-systolic dimensions divided by the end-diastolic size, was calculated to assess cardiac contractile function.

BUN assay. Serum blood urea nitrogen was measured in duplicate using the QuantiChrom Urea Assay Kit (BioAssay Systems) per the manufacturer's directions and assayed on the PolarStar Optima plate reader (BMG Labtech).

Spontaneous motion. Transgenic and age and sex-matched wild-type FVB mice (3, 9, and 13 months old) were individually housed in Oxymax/Comprehensive Lab Animal Monitoring System (CLAMS) chambers (Columbus Scientific). The spontaneous physical activity of the animals was quantified by the number of interruptions of the infrared beams emitted by photocells in the horizontal and vertical planes of the chambers. The experiments were conducted for 48 hours using regulated 12 hour day/night cycles, with normal feed conditions during the first 24 hours and fasted from food during the last 24 hours. Mice were provided water ad libitum during the entire experiment.

Exercise capacity. The exercise capacity of transgenic and age and sex-matched wild-type FVB mice was determined by measuring running time to exhaustion on a variable speed, multilane treadmill at a constant 10 degree angle (Exer-6M, Columbus Scientific). Mice were trained on by introducing them to the treadmill at slow speeds and once acclimated, running them under the test conditions. The next day the test was performed by first running the mice for 5 minutes at the initial speed of 10 meters per minute (m/min) and then the speed was increased by 1 m/min for each additional minute. The time the animals ran on the treadmill was recorded and the experiment stopped when the mice no longer avoided the mild electrical stimulus (intensity 8, repetition rate 4) on the platform at the end of the treadmill belt (intensity 8, repetition rate 4). The amount of work performed was calculated as work (Joules) = body weight (kg) × running speed (meters/min) × time (minutes) × grade (in degrees) × 9.8 (J/kg x m).[20]

Statistics. For the treadmill and Oxymax motion detection experiments, differences between the 2 groups were assessed using the two-tailed unpaired Student *t* test assuming equal variances (Microsoft Excel 2007). Differences in amyloid deposit formation between doxycycline-treated and control mice were assessed by χ^2 analysis using Microsoft Excel 2007.

Results

Generation of CMV-λ6 transgenic mice

Pronuclear injections of the linearized restricted pcDNA-AL080 λ6 cDNA expression construct (Figure 1A) produced 74 pups; 5 were positive for the transgene by PCR. This was confirmed by Southern blotting using probes to both the λ6 variable gene and bovine growth hormone polyadenylation sequence (data not shown). Three mice were able to pass the transgene to their offspring (Figure 1B), generating 3 lines (AL26, AL53, and AL55) that were transgenic for the λ6 LC and formally designated FVB-Tg(CMV-IGL6-AL080)26Dcs, FVB-Tg(CMV-IGL6-AL080)53Dcs, and FVB-Tg(CMV-IGL6-AL080)55Dcs.

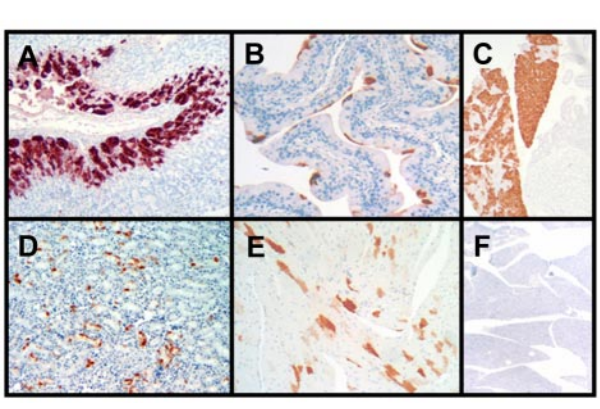

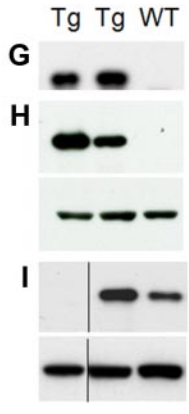

Figure 2. Expression of the human λ6 LC protein in CMV-λ6 transgenic mice. (A-F) Immunohistochemistry demonstrating human λ LC expression (red-brown staining) in (A) stomach, (B) bladder, (C) pancreas, (D) kidney, and (E) heart. (F) Pancreas stained with human κ LC antibody (negative control) is also shown. Antibodies used were Dako nos. A0193 (λ) and A0191 (κ). (G-I) Immunoblots of human λ LC expression (top panels) in serum (G), pancreas (H), and stomach (I) tissue extracts from transgenic (Tg) and wild-type (WT) littermate mice. β-actin was used as a loading control (H-I bottom panel). The anti–human λ antibody used was Sigma-Aldrich no. L5267. The vertical line indicates that noncontiguous lanes from the same immunoblot image are shown.

Transgene expression

Expression of the human λ LC protein in the transgenic mice was assessed by immunohistochemistry and immunoblot analysis of proteins extracted from organ homogenates. By immunohistochemistry, the human λ LC was detected in epithelial cells, including those lining the gastric glands of the stomach (Figure 2A), bladder (Figure 2B), the exocrine and endocrine pancreas (Figure 2C), tubular cells of the kidney (Figure 2D), columnar epithelial cells of the intestine and the cardiomyocytes of the heart in line AL26 only (Figure 2E). Human λ staining was also detected in the esophagus, trachea, prostate, testis, brain, and spinal cord, but not in the liver, lung, salivary glands, thymus, lymph nodes, fat, tongue, and bone marrow. The staining pattern was patchy in some organs but specific for the human λ LC, as antibodies to the human κ LC do not cross-react (Figure 2F), nor does the human λ antibody recognize endogenous mouse LC (data not shown). The immunohistochemistry data were confirmed by immunoblot analysis of protein extracts from organ homogenates using a different polyclonal anti–human λ LC antibody (Figure 2H-I); organs which had no detectable staining by immunohistochemistry (such as spleen) showed no detectable human λ LC by immunoblot. Organs from nontransgenic control littermates were also negative. Human λ LC was detected in serum (Figure 2G) and cerebrospinal fluid which was collected as described[21] (data not shown). The concentration of circulating human λ LC was estimated to be 5-10 mg/L by immunoblot comparison to known concentrations of LC; this concentration range is below the limit of detection by nephelometry (data not shown). Other than cardiac expression in line AL26, no other differences were detected between the 3 lines. Line AL55 mice were used for the experiments, unless otherwise noted.

Amyloid deposition

Tissues from transgenic mice at various ages from each of the 3 transgenic lines were examined for the presence of Congo red-staining fibrillar deposits using polarized light microscopy. Amyloid deposits were found in the lumen of the gastric glands of the stomach of mice of each of the transgenic lines (Figure 3A-B). Often, the stomach epithelium was dysplastic and formed polyps and dilated glands filled with Congophilic material. Immunohistochemical examination of the intraluminal material and the surrounding gastric epithelial cells demonstrated positive staining for human λ LC (Figure 3C), but not for the control human κ LC (Figure 3D). Electron microscopic examination confirmed that the luminal contents contained unbranched fibrils with a diameter of 10 nm, observations consistent with amyloid (Figure 3E). Congophilic deposits were not detected in any other organ examined, up to age 24 months. Fibril deposition increased with age: approximately 26% of the mice aged 6 months and younger had Congophilic deposits in the stomach when single sections were examined, but by 24-30 months of age, 83% of mice had deposits, which were not detected in the stomachs of aged wild-type littermates (Figure 4).

Amyloid fibrils were isolated from pooled samples of stomachs that were confirmed to have amyloid fibrils by Congo red staining of paraffin sections. Water wash-extracted fibrils[17] were confirmed to contain human λ LC by immunoblotting (data not shown). As a further confirmation that the Congo red-staining deposits in the lumens of the gastric glands were made up of human λ LC protein, the amyloid deposits were isolated using laser capture microdissection (LCM). The solubilized proteins from the deposit were heterogeneous by silver stain on a 10%-15% gradient acrylamide gel, with an intense band corresponding to the size of the human λ LC (data not shown). Immunoblot analysis confirmed that the human λ LC was present in the microdissected deposits (Figure 3F).

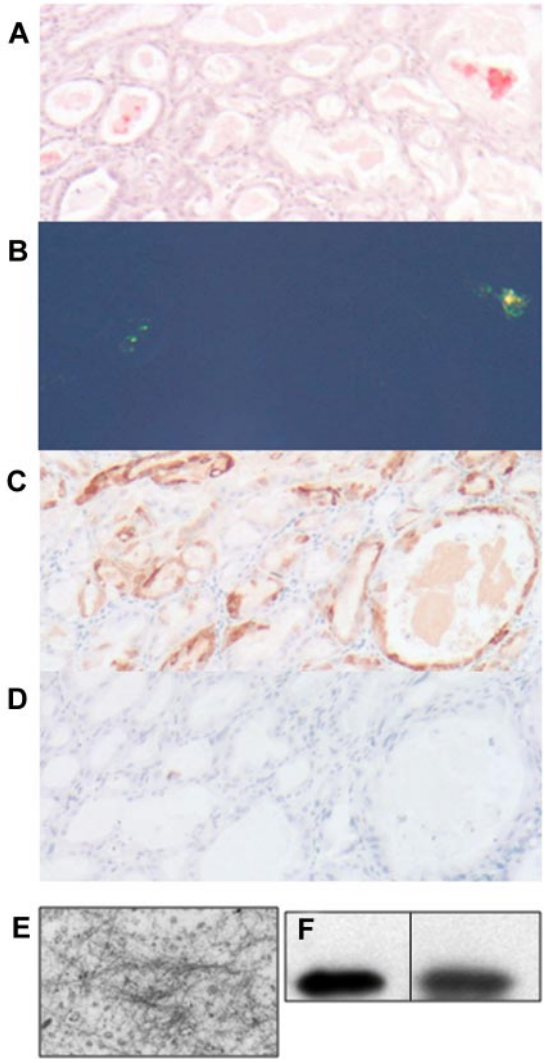

Figure 3. Amyloid deposits in the stomach of CMV-λ6 transgenic mice. Stomach sections were stained with Congo red and counterstained with hematoxylin visualized by brightfield (A) or polarized light microscopy (B). (C-D) Demonstration of immunohistochemical staining with anti–human λ and anti–human κ LC, respectively. (E) Negative staining EM of the contents of the stomach glands in the stomach of a transgenic mouse with Congo red positive deposits. Fibril diameters are approximately 10 nm. (F) Immunoblot for human λ LC in protein extracted from stomach amyloid deposits isolated by LCM (lane 1); serum from a transgenic mouse as a control (lane 2). The vertical line indicates that noncontiguous lanes from the same immunoblot image are displayed.

Neurologic phenotype

As the transgenic mice aged, approximately 20% of the mice developed a neurologic phenotype characterized by a gait disturbance and limb clenching when the mice were picked up by the tail. This limb clenching behavior has been reported in transgenic mouse models of neurodegenerative diseases.[22]

The spontaneous motion of old mice (13 months) who displayed the limb clenching phenotype was assessed using the CLAMS system. Under normal feeding conditions, spontaneous activity was similar between the transgenic mice and control. Likewise, under fasting conditions during the day, the activity was

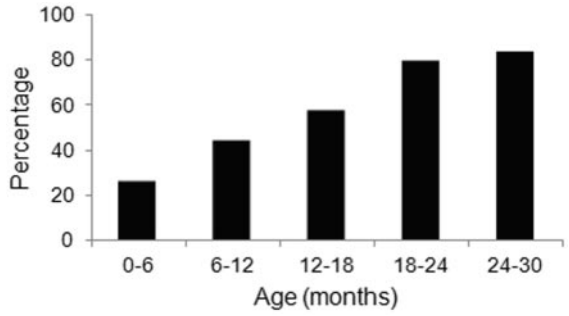

Figure 4. Age-dependent increase in amyloid deposition in CMV-λ6 mice. Proportion of transgenic mice at various ages with amyloid deposits in stomach sections detected by Congo red staining of a single section of stomach. Groups included mice that were < 6 months (n = 19), 6-12 months (n = 18), 12-18 months (n = 54), 18-23 months (n = 29), and 24-30 months of age (n = 6).

comparable. However, under fasting conditions at night (when the mice are actively searching for food), the transgenic mice displayed significantly less spontaneous motion, particularly in the vertical (rearing) direction ($P < .0068$; Figure 5A).

The ability of the transgenic mice to run on an inclined treadmill was compared with that of age-matched wild-type control mice at 3 and 9 months of age. Although younger age (3 months) transgenic and control mice displayed similar exercise capacity (data not shown), older CMV-λ6 mice demonstrated significant impairment in their ability to run for extended times (mean 9.5 minutes vs 15.3 minutes, $P < .007$) and performed significantly less work (Figure 5B, mean 178.7 J vs 315.4 J, $P < .011$).

The neurologic phenotype was correlated with neuropathologic findings at necropsy. We found that the transgenic mice express the human LC sporadically in cells of the brain. In addition, we identified neurons with dystrophic axons in the spinal cord and medulla (Figure 5C).

Other organ dysfunction

Many patients with AL amyloidosis develop cardiac and renal dysfunction, which may be caused by a combination of fibrillar protein deposition and acute toxicity mediated by prefibrillar aggregates.[23,24] Although we did not observe amyloid deposits in the heart or kidneys of transgenic mice, organ function was assessed to determine whether there was any evidence of toxicity because of circulating LC. Cardiac function and the thickness of heart walls and septums were measured by echocardiography. Ejection fraction, fractional shortening, heart rate and thickness of the interventricular septum and left ventricle size were similar between the transgenic mice and wild-type littermate controls, including line AL26 which has cardiac expression of the LC. With respect to renal dysfunction, there was no increase in total urinary protein secretion or blood urea nitrogen (BUN) levels in the transgenic mice compared with their wild-type littermates.

Doxycycline inhibition of amyloid fibril formation

CMV-λ6 transgenic mice develop amyloid deposits in the stomach with age, with 26% of the mice having deposition by 6 months. Transgenic mice of 3-6 months of age, (when 20%-25% of mice would be expected to have amyloid deposits) were treated with doxycycline in the drinking water to determine whether treatment would prevent further deposition. After oral treatment for at least 7 months, 23% (4/17) of the treated mice had Congo red positive deposits in the stomach, compared with 69% (11/16) of the untreated controls, $P = .00006$ (χ^2 analysis; Figure 6A-B).

Doxycycline disrupts amyloid in vitro

Recombinant amyloidogenic LC samples were incubated with doxycycline or water alone, then subjected to cycles of heating and shaking to generate amyloid fibrils in vitro. The formation of fibrils was visualized by negative stain transmission electron microscopy. As soon as 24 hours, LC under control conditions began to aggregate and form protofibrils. This process was inhibited by the presence of doxycycline, which reduced the number of protofibrils seen and increased formation of disordered aggregates, in a dose-dependent manner. By 4 days of incubation, many short, mature fibrils were observed in the absence of drug whereas small, broken pieces of fibrils and aggregates were observed with doxycycline. Images are shown that were obtained at the end of the experiment, after 5 days of incubation. In water, the recombinant LC formed mature and intact amyloid fibrils (Figure 6C), whereas in the presence of doxycycline, the fibrils that resulted were disorganized, broken, and had frayed ends (Figure 6D-E). Both the high and low concentrations of doxycycline disrupted amyloid fibrils, with the higher dose having a greater effect. A second

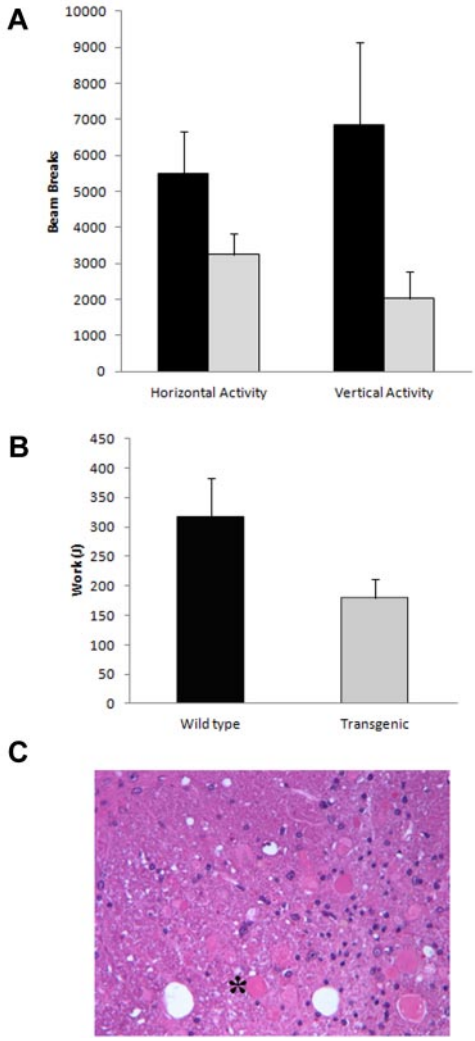

Figure 5. Neurologic phenotype in CMV-λ6 mice. (A) The transgenic mice displayed less spontaneous activity compared with wild-type controls when fasted overnight ($P < .018$ horizontal, $P < .0068$ vertical, n = 4 each group). (B) Exercise capacity on an inclined treadmill was diminished in older transgenic mice compared with age-matched controls ($P < .011$, n = 4 each group). (C) H&E-stained section of spinal cord revealing dystrophic neurons (example denoted as *) in an old transgenic mouse with the limb clenching phenotype.

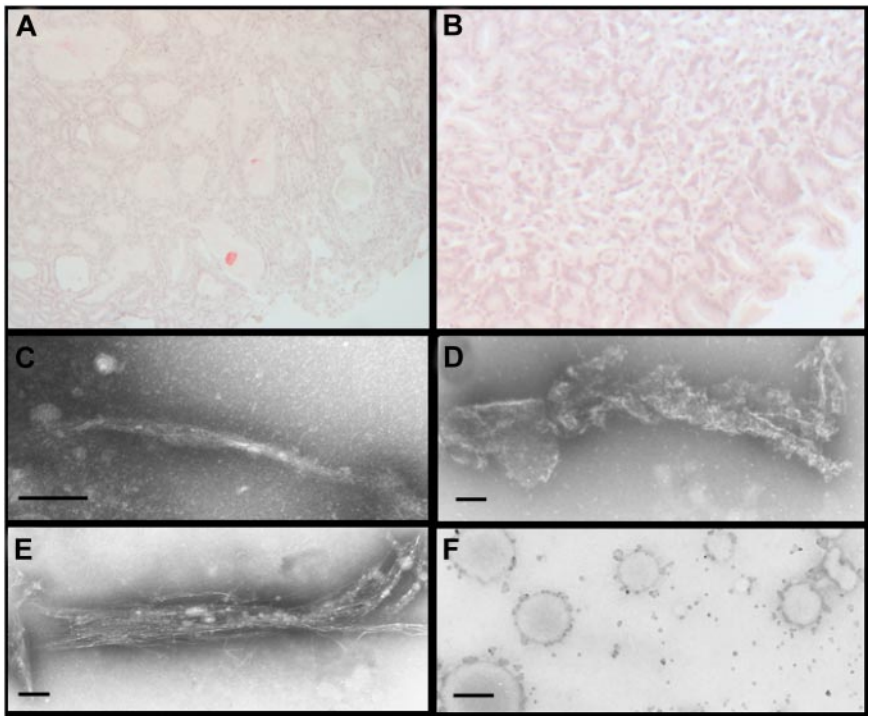

Figure 6. Doxycycline prevents amyloid deposition in vivo and directly interacts with LC in vitro. (A) In control CMV-λ6 transgenic mice drinking water alone, 69% (11/16) had Congo red positive deposits in the stomach. (B) Deposits were inhibited by oral administration of doxycycline in the drinking water, identified in only 23% (4/17) of the treated mice ($P = .00006$, χ^2 analysis). (C) For a 5-day period of incubation, recombinant amyloidogenic LC in vitro form typical amyloid fibrils, as visualized by negative stain TEM, (D) whereas incubation with 250 mg/L doxycycline resulted in degraded and broken fibrils and disorganized bundles of immature fibrils (data not shown). (E) With 15 mg/L doxycycline, broken fibrils with frayed ends were observed. (F) Amyloid fibrils extracted from autopsy material formed numerous large aggregates after incubation with doxycycline. (C-E) Magnification ×42 000, bar = 100 nm; magnification ×10 000, bar = 500 nm.

independent experiment gave similar results. To test the effect of doxycycline on patient fibrils ex vivo, amyloid fibrils were extracted from autopsy tissue obtained from the patient from which the transgene was derived and incubated with doxycycline. Numerous large aggregates were detected after incubation of tissue-extracted fibrils with doxycycline, confirming a direct interaction between the drug and the fibrils (Figure 6F).

Discussion

We have developed a transgenic mouse model in which expression of a full-length human amyloidogenic Ig LC reproducibly and consistently produces amyloid deposition in the stomach. The LC variable region is derived from the λ6 germ line gene family, a variable gene rarely used in the normal expressed repertoire but detected in approximately 18% of patients with AL amyloidosis.[25] To our knowledge, this is the first report of transgenic mice developing fibrillar deposits of human amyloidogenic Ig LC. Amyloid can form in the kidney of mice after injection of > 5 g of purified human urinary LC,[11] but this model is not practical for serial studies of disease and treatment. As an alternative, we developed a model in which the LCs are continuously produced by implanted stably transfected plasmacytoma cells secreting an amyloidogenic human LC.[26] Although this model obviates the need to purify protein for injection, it is limited by the size of the plasmacytoma, and can typically be used for 4-6 weeks. In this time frame, circulating amyloidogenic LCs have acute effects on the renal and cardiac system, as well as inducing a potentially protective response in an increase of the redox sensitive heme oxygenase-1 protein in the heart, originally described in treated primary cardiomyocytes.[4] Amorphous LC deposits occur in the kidney tubules of mice implanted with plasmacytoma cells that were transfected with 3 different patient-derived LC genes (2 λ6 and 1 κ1). These experiments have been carried out in syngeneic wild-type mice and repeated in RAG1$^{-/-}$ (recombinase activating gene) mice, which do not mount an immune response because of a lack of B and T lymphocytes.

The expression of a human LC in mice from birth prevents the mouse immune system from identifying the human LC as a foreign protein. Consequently the LC is present for the entire lifetime of the mouse. Using the CMV promoter, LC were expressed mainly in epithelial organs and low levels of human LC were detected in the serum at levels comparable with healthy people, although in this case the human LC is a single clonal species and amyloidogenic. The CMV-λ6 transgenic mice develop amyloid deposits at a local site in the lumen of the stomach. Amyloid in the stomach is not a frequent manifestation of disease, but has been reported.[27,28] Factors that promote fibrillogenesis at this site may include the local concentration of LC or the acidic environment of the stomach; acidic conditions promote fibrillogenesis in vitro.[29] The Congophilic material in the transgenic mouse stomach was confirmed to have the ultrastructural characteristics of amyloid including unbranched fibrils of 10 nm diameter when examined by electron microscopy. As expected, the fibrils were composed of human λ LC by immunohistochemistry and immunoblot analysis of the extracted and laser microdissected fibrils. Mass spectrometry[30] has not been done but would undoubtedly be confirmatory.

In some transgenic models, overexpressed amyloidogenic proteins may interact with the endogenous wild-type protein. In human transthyretin (TTR) transgenics, the mice can form hybrid tetramers of human mutant and wild-type mouse TTR subunits; this process is thought to stabilize the mutant protein.[31] Alternatively, interactions of transgenic and endogenous proteins may promote fibril formation, as in prion transgenic mice.[32] However, in the case of the CMV-λ6 transgenic mice, this situation does not appear to be the case as the transgenic mouse has been crossed to the RAG1$^{-/-}$ background, which has no endogenous mouse Ig heavy or LC, and no alteration was observed on phenotype (data not shown).

In TTR transgenic mice, expression and phenotype do not always parallel the disease in humans. This could be a result of differences in accessory molecule expression in mice such as

glycoaminoglycans, or other tissue-specific factors. The strain of the mouse is also a potential modifying factor in TTR transgenic mice, with some strains being protective and others promoting amyloid formation.[33] C57/BL6 mice were more susceptible to disease caused by expression of a mutant human TTR transgene. We have bred the CMV-λ6 transgene into the C57/BL6 background and have observed no increase in fibrillogenesis, so this strain may not promote the AL phenotype (data not shown).

In AL amyloidosis, the amyloidogenic LCs are produced by clonal bone marrow plasma cells. The use of a B cell specific transgenic promoter might more faithfully recapitulate this process, but a previously reported attempt to express a λ LC transgene found that premature LC expression blocked early B cell development.[34] We used the human CMV immediate early promoter in an attempt to achieve high local concentrations of LC in target organs. Different transgenic mice using the immediate early CMV promoter have displayed diverse transgenic expression patterns that have not generally been as ubiquitous as the promoter when expressed in tissue culture cells. Although gene expression with the CMV promoter in transgenic mice has been reported in a variety of epithelial organs, exocrine organs, heart or skeletal muscle, brain and testis, protein production is often restricted to certain cells types in these organs.[35-37] One of the 3 lines (AL26) had expression of the λ LC protein in the heart by immunoblot analysis, and IHC further identified that the LC was expressed in the muscle cells of the heart. Nonetheless, no cardiac phenotype was observed in these mice.

Approximately 20% of the CMV-λ6 mice displayed hind limb clenching, gait disturbance, and ataxia corresponding to dystrophic neurons in the medulla and spinal cord of older mice. Patients with AL amyloidosis can develop peripheral and/or autonomic neuropathy.[38] Axonal degeneration, usually without demyelination, has been observed in areas where amyloid deposits are located in the proximal dorsal root and sympathetic ganglia, peripheral nerves, epineural and endoneurial connective tissue, and around the endoneurial microvessels.[39] It has been hypothesized that neuropathy could be a result of physical compression of the nerve by amyloid deposits or the consequence of ischemia because of perivascular amyloid deposits. In our transgenic mouse model, no amyloid fibrils were detected in the brain, spinal cord, or peripheral nerves. However, LC were produced by some cells in the medulla and spinal cord, and human LC was detected in the CSF by immunoblotting (data not shown). Toxic prefibrillar LC could contribute to the axonal dystrophy. Dystrophic axons are a hallmark of Alzheimer pathology[40] and may arise from a disruption of axonal motor transport.[41] The limb clenching phenotype observed in out transgenic mice has also been observed in other mouse models of neurodegeneration and axonal transport disruption, such as with mutations in the dynein motor protein.[22,42] Further study is warranted to investigate the neurotoxic effects of nonfibrillar species, as neuropathology has been understudied in AL amyloidosis and could be an early marker of disease progression.[43]

The deposition of amyloid in the lumen of the gastric glands of the stomach allows the model to be used to test potential oral therapeutics. We analyzed the ability of doxycycline to inhibit amyloid fibril formation, based on the previous observations by Cardoso et al in an FAP transgenic mouse model.[44,45] The frequency of mice with amyloid deposits was significantly decreased in CMV-λ6 mice receiving doxycycline in their drinking water. Tetracyclines, including the derivative doxycycline, have been shown in vitro to inhibit amyloid fibrillogenesis, cause disruption of fibrils, and produce noncytotoxic aggregates with TTR and Aβ peptides.[46,47] In our study, we present evidence that doxycycline interacted with LC in vitro causing disruption of fibril formation in the recombinant LC experiment and degradation of mature LC fibrils extracted from tissue. Doxycycline was studied at 2 concentrations in vitro, 250 mg/L, which is half the concentration of the drug in the mouse water bottles, and 15 mg/L, the human serum concentration achieved with the standard prescribed dosage of doxycycline.[48] Results with doxycycline were similar for both the fibril formation experiments and testing of the ex vivo fibrils, ie fibrils were disrupted at both concentrations of drug, with the higher concentration having the most effect. Doxycycline is also an inhibitor of matrix metalloproteinases (MMP), including MMP-9, an important contributor to extracellular matrix (ECM) remodeling. MMP-9 has been reported to be elevated in the serum, heart, and kidneys of patients with AL amyloidosis; levels are elevated in the stomachs of these transgenic mice with amyloid deposits (data not shown), and MMPs may contribute to the pathogenesis of amyloid-induced organ damage.[49,50] Thus, treatment with doxycycline may be beneficial through multiple mechanisms. Further investigation of doxycycline and tetracycline derivatives may be warranted in AL amyloidosis to determine whether such compounds can inhibit amyloid formation at other sites. Drug effectiveness will depend on bioavailability and possibly tissue-specific factors. If efficacious, doxycycline may offer a much needed therapeutic targeted to the amyloid deposits, which in combination with existing antiplasma cell therapies, may offer a more complete approach to the eradication of this devastating disease.

In conclusion, we have generated a transgenic mouse model that forms amyloid deposits composed of human Ig LC. This model will be useful for the study of local factors that affect amyloidogenesis, including tissue factors such as pH, and locally acting accessory molecules and cofactors such as chaperones. Furthermore, the presence of amyloid in the stomach has made this model useful for studying orally available drugs and dietary supplements that could alter amyloid formation in this site. We have successfully used this model to assess the antifibril properties of doxycycline. Based on these results, doxycycline or other tetracycline analogs should be considered for testing in patients with AL amyloidosis through controlled clinical trials, as is being done in other systemic amyloidoses.

Acknowledgments

The authors thank Greg Martin and Dr Katya Ravid of the BU Transgenic core facility; Kristina Perry and Dr Pamela Larson from Dr Carol Rosenberg's laboratory for assistance with LCM; Maria Perez of the BUSM LASC for insightful observations; Dr Roderick Bronson from the Harvard Rodent Histopathology Core for helpful discussions; Drs Kaori Sato and Kenneth Walsh for echocardiography; Varuna Shibad for technical assistance; and Dr Elena Klimtchuk and Gloria Chan for recombinant LC; and Kate Bailey, Tucker Berk, Michael Greene and Brian Spencer of the Gerry Amyloid Laboratory for technical assistance.

This work was funded by a P01 from NHLBI HL68705-04, gifts from the Gruss Foundation and the Wildflower Foundation, and support from the Solimando Fund to J.E.W.

Authorship

Contribution: J.E.W. designed and performed research, interpreted data, and wrote the paper; R.R. performed the electron microscopy

and interpreted data; G.T. designed and performed research and analysis of the motion and treadmill studies; P.S. performed the histology; J.G. performed the echocardiography and interpreted data; C.O. analyzed histology; R.J. designed and analyzed the motion and treadmill studies; V.T.-R. interpreted data and discussed the paper; R.L. interpreted data and discussed the paper; L.H.C. participated in writing the paper; and D.C.S. designed research, interpreted data, and wrote the paper.

Conflict-of-interest disclosure: The authors declare no competing financial interests.

Correspondence: David C. Seldin, MD, PhD, 72 E Concord St, Boston, MA 02118; e-mail:dseldin@bu.edu.

References

1. Merlini G, Seldin DC, Gertz MA. Amyloidosis: pathogenesis and new therapeutic options. *J Clin Oncol.* 2011;29(14)1924-1933.
2. Kisilevsky R. Proteoglycans, glycosaminoglycans, amyloid-enhancing factor, and amyloid deposition. *J Intern Med.* 1992;232(6):515-516.
3. Pepys MB, Tennent GA, Booth DR, et al. Molecular mechanisms of fibrillogenesis and the protective role of amyloid P component: two possible avenues for therapy. *Ciba Found Symp.* 1996; 19973-19981.
4. Brenner DA, Jain M, Pimentel DR, et al. Human amyloidogenic light chains directly impair cardiomyocyte function through an increase in cellular oxidant stress. *Circ Res.* 2004;94(8):1008-1010.
5. Liao R, Jain M, Teller P, et al. Infusion of light chains from patients with cardiac amyloidosis causes diastolic dysfunction in isolated mouse hearts. *Circulation.* 2001;104(14):1594-1597.
6. Monis GF, Schultz C, Ren R, et al. Role of endocytic inhibitory drugs on internalization of amyloidogenic light chains by cardiac fibroblasts. *Am J Pathol.* 2006;169(6):1939-1952.
7. Trinkaus-Randall V, Walsh MT, Steeves S, Monis G, Connors LH, Skinner M. Cellular response of cardiac fibroblasts to amyloidogenic light chains. *Am J Pathol.* 2005;166(1):197-208.
8. Kayed R, Head E, Thompson JL, et al. Common structure of soluble amyloid oligomers implies common mechanism of pathogenesis. *Science.* 2003;300(5618):486-489.
9. Reixach N, Deechongkit S, Jiang X, Kelly JW, Buxbaum JN. Tissue damage in the amyloidoses: Transthyretin monomers and nonnative oligomers are the major cytotoxic species in tissue culture. *Proc Natl Acad Sci U S A.* 2004;101(9):2817-2822.
10. Walsh DM, Selkoe DJ. Oligomers on the brain: the emerging role of soluble protein aggregates in neurodegeneration. *Protein Pept Lett.* 2004; 11(3):213-228.
11. Solomon A, Weiss DT, Pepys MB. Induction in mice of human light-chain-associated amyloidosis. *Am J Pathol.* 1992;140(3):629-637.
12. Hovey BM, Ward JE, Soo Hoo PT, O'Hara CJ, Connors LH, Seldin DC. Preclinical development of siRNA therapeutics for AL amyloidosis [published online ahead of print May 12, 2011]. *Gene Therapy.* doi:10.1038/gt.2011.69.
13. Welschof M, Terness P, Kolbinger F, et al. Amino acid sequence based PCR primers for amplification of rearranged human heavy and light chain immunoglobulin variable region genes. *J Immunol Methods.* 1995;179(2):203-214.
14. Gozal YM, Cheng D, Duong DM, Lah JJ, Levey AI, Peng J. Merger of laser capture microdissection and mass spectrometry: a window into the amyloid plaque proteome. *Methods Enzymol.* 2006; 41277-41293.
15. Klimtchuk ES, Gursky O, Patel RS, et al. The critical role of the constant region in thermal stability and aggregation of amyloidogenic immunoglobulin light chain. *Biochem.* 2010;49(45):9848-9857.
16. Baden EM, Owen BA, Peterson FC, Volkman BF, Ramirez-Alvarado M, Thompson JR. Altered dimer interface decreases stability in an amyloidogenic protein. *J Biol Chem.* 2008;283(23): 15853-15860.
17. Skinner M, Shirahama T, Cohen AS, Deal CL. The association of amyloid P-component (AP) with the amyloid fibril: an updated method for amyloid fibril protein isolation. *Prep Biochem.* 1982;12(5):461-476.
18. Ren R, Hong Z, Gong H, et al. Role of glycosaminoglycan sulfation in the formation of immunoglobulin light chain amyloid oligomers and fibrils. *J Biol Chem.* 2010;285(48):37672-37682.
19. Liao R, Jain M, Cui L, et al. Cardiac-specific overexpression of GLUT1 prevents the development of heart failure attributable to pressure overload in mice. *Circulation.* 2002;106(16):2125-2131.
20. Pederson BA, Cope CR, Irimia JM, et al. Mice with elevated muscle glycogen stores do not have improved exercise performance. *Biochem Biophys Res Commun.* 2005;331(2):491-496.
21. DeMattos RB, Bales KR, Parsadanian M, et al. Plaque-associated disruption of CSF and plasma amyloid-beta (Abeta) equilibrium in a mouse model of Alzheimer's disease. *J Neurochem.* 2002;81(2):229-236.
22. Holzbaur EL. Motor neurons rely on motor proteins. *Trends Cell Biol.* 2004;14(5):233-240.
23. Falk RH, Dubrey SW. Amyloid heart disease. *Prog Cardiovasc Dis.* 2010;52(4):347-361.
24. Shi J, Guan J, Jiang B, et al. Amyloidogenic light chains induce cardiomyocyte contractile dysfunction and apoptosis via a non-canonical p38alpha MAPK pathway. *Proc Natl Acad Sci U S A.* 2010; 107(9):4188-4193.
25. Prokaeva T, Spencer B, Doros G, Connors LH, Skinner M, Seldin DC. Contribution of light chain variable region genes to organ tropism and survival in AL amyloidosis. *Amyloid.* 2010;17(S1):62.
26. Ward JE, Brenner D, SooHoo P, et al. Mouse models of AL amyloidosis. In: Skinner M, Berk JL, Connors LH, Seldin DC, eds. *XIth International Symposium of Amyloidosis.* Boca Raton, FL: Taylor & Francis; 2008:321-323.
27. Marques M, Sarmento JA, Rodrigues S, Guimaraes S, Fonseca E, Macedo G. Gastric amyloidosis: unusual cause of upper gastrointestinal hemorrhage. *Endoscopy.* 2011;43(suppl 2E): 100-101.
28. Shuttleworth E, Keld R, Willert R, Benbow EW. Amyloidosis: an EUS view [published online ahead of print April 4, 2011]. *Gastrointest Endosc.* doi:10.1016/j.gie.2011.01.039.
29. Khurana R, Gillespie JR, Talapatra A, et al. Partially folded intermediates as critical precursors of light chain amyloid fibrils and amorphous aggregates. *Biochem.* 2001;40(12):3525-3535.
30. Vrana JA, Gamez JD, Madden BJ, Theis JD, Bergen HR 3rd, Dogan A. Classification of amyloidosis by laser microdissection and mass spectrometry-based proteomic analysis in clinical biopsy specimens. *Blood.* 2009;114(24):4957-4959.
31. Reixach N, Foss TR, Santelli E, Pascual J, Kelly JW, Buxbaum JN. Human-murine transthyretin heterotetramers are kinetically stable and non-amyloidogenic: a lesson in the generation of transgenic models of disease involving oligomeric proteins. *J Biol Chem.* 2008;283(4):2098-2107.
32. Maeda S. Mouse models of amyloidoses generated by transgenesis. *Amyloid.* 1996;3214-3215.
33. Teng M, Buxbaum JN. Transgenic mice in amyloid research: an interpretive review. *Amyloid.* 1996;3187-3208.
34. Levinson DA, Campos-Torres J, Leder P. Molecular characterization of transgene-induced immunodeficiency in B-less mice using a novel quantitative limiting dilution polymerase chain reaction method. *J Exp Med.* 1993;178(1):317-329.
35. Baskar JF, Smith PP, Ciment GS, et al. Developmental analysis of the cytomegalovirus enhancer in transgenic animals. *J Virol.* 1996;70(5):3215-3226.
36. Baskar JF, Smith PP, Nilaver G, et al. The enhancer domain of the human cytomegalovirus major immediate-early promoter determines cell type-specific expression in transgenic mice. *J Virol.* 1996;70(5):3207-3214.
37. Zhan Y, Brady JL, Johnston AM, Lew AM. Predominant transgene expression in exocrine pancreas directed by the CMV promoter. *DNA Cell Biol.* 2000;19(11):639-645.
38. Benson MD, Kincaid JC. The molecular biology and clinical features of amyloid neuropathy. *Muscle Nerve.* 2007;36(4):411-423.
39. Kyle RA, Kelly JJ, Dyck PJ. Neuropathy Associated with Malignancy: 108: Amyloidosis and Neuropathy. In: Dyck PJ, Thomas PK, eds. *Peripheral Neuropathy* (4th ed). Philadelphia, PA: W.B. Saunders; 2005:2427-2451.
40. Fiala JC. Mechanisms of amyloid plaque pathogenesis. *Acta Neuropathol.* 2007;114(6):551-571.
41. Stokin GB, Goldstein LS. Axonal transport and Alzheimer's disease. *Annu Rev Biochem.* 2006; 75607-75627.
42. Hafezparast M, Klocke R, Ruhrberg C, et al. Mutations in dynein link motor neuron degeneration to defects in retrograde transport. *Science.* 2003; 300(5620):808-812.
43. Duston MA, Skinner M, Anderson J, Cohen AS. Peripheral neuropathy as an early marker of AL amyloidosis. *Arch Intern Med.* 1989;149(2): 358-360.
44. Cardoso I, Martins D, Ribeiro T, Merlini G, Saraiva MJ. Synergy of combined Doxycycline/TUDCA treatment in lowering Transthyretin deposition and associated biomarkers: studies in FAP mouse models. *J Transl Med.* 2010;8:74.
45. Cardoso I, Saraiva MJ. Doxycycline disrupts transthyretin amyloid: evidence from studies in a FAP transgenic mice model. *FASEB J.* 2006;20(2): 234-239.
46. Cardoso I, Merlini G, Saraiva MJ. 4′-iodo-4′-deoxydoxorubicin and tetracyclines disrupt transthyretin amyloid fibrils in vitro producing noncytotoxic species: screening for TTR fibril disrupters. *Faseb J.* 2003;17(8):803-809.
47. Forloni G, Colombo L, Girola L, Tagliavini F, Salmona M. Anti-amyloidogenic activity of tetracyclines: studies in vitro. *FEBS Lett.* 2001;487(3): 404-407.
48. Agwuh KN, MacGowan A. Pharmacokinetics and pharmacodynamics of the tetracyclines including glycylcyclines. *J Antimicrob Chemother.* 2006; 58(2):256-265.
49. Biolo A, Ramamurthy S, Connors LH, et al. Matrix metalloproteinases and their tissue inhibitors in cardiac amyloidosis: relationship to structural, functional myocardial changes and to light chain amyloid deposition. *Circ Heart Fail.* 2008;1(4): 249-257.
50. Keeling J, Herrera GA. Matrix metalloproteinases and mesangial remodeling in light chain-related glomerular damage. *Kidney Int.* 2005;68(4):1590-1603.